WOOD SORPTION FRACTALITY IN THE HYGROSCOPIC RANGE. PART II. NEW MODEL DEVELOPMENT AND VALIDATION[1]

Bingye Hao[2]
Former Ph.D. student

and

Stavros Avramidis†
Professor
Department of Wood Science
The University of British Columbia
Vancouver, BC, V6T 1Z4 Canada

(Received April 2003)

ABSTRACT

The sorption isotherms of mature sapwood and heartwood from two softwood species were obtained experimentally. The data were used for the determination of how their fractal values change with an increase in moisture content using the *Hao-Avramidis* model developed in the past, and for the substantiation of a new fractal polynomial sorption equation based mainly on the fractal parameter *D*, assuming *D* being the dominant control parameter of sorption at higher sorption regions. The new sorption theory considered both the molecular layering stage at low humidities and the non-layering or fractal sorption stages at high humidities. Its good curve-fitting behavior justified the assumption that the state dynamics of the sorbed water were stepwise or locative instead of smooth, and three or four steps were identified.

Keywords: Water, sorption, isotherm, fractal dimension, internal surface.

INTRODUCTION

In a recent paper by Hao and Avramidis (2001), the modified classic BET sorption equation (referred to as the *HA* model) was developed based on the principles of a non-homogeneous sorption surface and the fractal analysis approach, and thereafter, was validated with sorption data from Kelsey (1957). A new sorption parameter—fractal dimension, *D*—was introduced for describing the quantitative changes in spatial organization of the sorbed water molecules within the cell walls with increasing moisture content, *M*. The *D*-*M* plots were used for providing more meaningful sorption information in relation to water molecular distribution within cell walls than the to date commonly used sorption isotherms (*M*-*h* plot, *h* referred to as relative vapor pressure).

In this paper, four wood types from two softwood species were used for the determination of how their *D* values change with an increase in *M* using the *HA* model, and for the validation of a newly derived sorption equation that is based mainly on the fractal value *D*, by assuming that *D* is the dominant control parameter of water sorption by wood at high moisture contents.

MATERIALS AND METHODS

Green samples of Douglas-fir (*Pseudotsuga menziesii* (Mirb.) Franco) and western red cedar (*Thuja plicata* Donn) were cut from freshly harvested logs. Each group was further separated into two types of wood, namely, Douglas-fir sapwood (DFS), Douglas-fir heartwood (DFH), western red cedar heartwood (RCH),

† Member of SWST.

[1] This project was funded by a Natural Sciences and Engineering Research Council of Canada Research Grant.

[2] Current address: 3269 School Ave., Vancouver, BC V5R 5N6, Canada.

and extracted western red cedar heartwood (E-RCH). Ten specimens (wafers of 30-mm × 20-mm × 2-mm thickness) from each wood type were cut with a micro-saw, so that their thickness direction was aligned with the tree's tangential direction. Each specimen contained 7~10 annual rings that were parallel to each other and parallel to the side edges. The specimens were free of visual defects and had smooth surfaces. Small thickness was used to facilitate the rapid establishment of equilibrium. In addition, the utilization of such thin specimens made the rapid removal of extractives possible without adversely affecting the wood substance.

Methanol was used to remove volatile and nonvolatile extractives in E-RCH specimens. Twenty RCH wafers were extracted in a soxhlet apparatus for about 12 h. The extraction continued until the solution surrounding the samples in the apparatus was visibly free of color from dissolved extractives. This was followed by distilled water extraction for 4 h. The extracted samples were then washed several times with hot distilled water. After these three steps, the initial extractives content of the wafers was measured to be 9.5%. The extractive-free specimens were wrapped in wet cloth to limit drying before the sorption study.

The sorption tests were carried out in two conditioning chambers (Parameter Generation & Control models 4-PC and 9-SS). Each chamber created a stable climate with an accuracy of ±1% in relative humidity and ±1°C in air temperature. The calculation of the relative vapor pressure (h) was based on direct dry-bulb and wet-bulb readings from RTDs placed in the chamber. Each specimen was placed in a weighing bottle. The procedure of sorption measurement followed a stepwise mode at three temperature levels, namely, 30, 40, and 50°C. For each temperature, the measurement was started with desorption (green specimens) where h ranged throughout this study from about 0.96 to 0.06. The lowest h value of 0.06 was created by a LiCl saturated solution. The specimens were placed above the solution in a desiccator, which in turn was placed in the conditioning chamber for temperature control. A magnetic stirrer was used for elimination of the formation of a water film on the surface of the solution.

After completion of the desorption sequence, the specimens were transferred to a vacuum oven at 70°C until oven-dry weight was reached. Since the RCH specimens were not extracted, they were vacuum dried at about 45°C in order to minimize removal of volatile extractives. The specimens remained in the oven for one week, and they were then moved into the conditioning chamber for the adsorption sequence. The weight of the bottle and specimen was measured by using a digital balance with a precision of 0.0001 g.

The experimental sorption isotherms were used to compute the D values for these four types of wood using the *HA* model (Hao and Avramidis 2001) shown as,

$$M = \frac{M_m c \sum_{n=1}^{n_{\max}} \left(h^n n^{D-2} \sum_{m=1}^{n} m^{2-D} \right)}{1 + c \sum_{n=1}^{n_{\max}} (h^n n^{D-2})} \quad (1)$$

where D = fractal dimension; M = equilibrium moisture content, %; M_m = monolayer sorption capacity, %; c = a constant related to the heat of sorption; n = number of water molecule layers; n_{max} = maximum possible number of layers of the sorbed water molecules in wood; and h = relative vapor pressure.

The calculated D values were found to exhibit a stepwise arrangement throughout the sorption isotherm. The following grouping guidelines were used for the grouping of the D values based on fractal properties,

$\boldsymbol{D} \leq 1.9$ (between a line and a surface)
$1.9 < \boldsymbol{D} \leq 2.2$ (about a planar surface)
$2.2 < \boldsymbol{D} \leq 2.3$ (formation of a rough surface begins)
$2.3 < \boldsymbol{D} \leq 2.5$ (rougher surface)
$\boldsymbol{D} > 2.5$ (towards a spatial filling)

The calculated D values from Eq. (1) for each sorption isotherm could be positioned

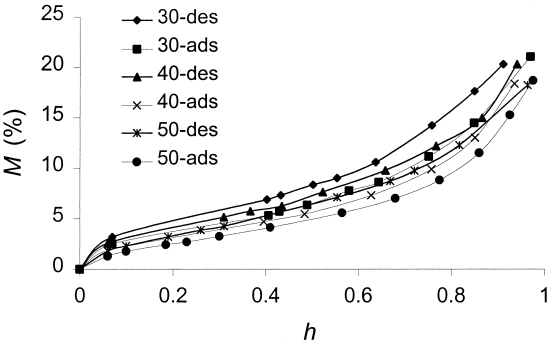

FIG. 1. Experimentally obtained sorption isotherms for Douglas-fir heartwood.

into three or four of the above groups, thus indicating a multi-fractal condition within the cell walls with respect to the sorbed water molecules. In terms of fractal property, a fractal object can essentially be represented by a single D value and the multi-fractal term could be simply quantified as the summation of individual fractal terms,

$$M_{fractal} = \Sigma k_i h^{D_i} \tag{2}$$

where $M_{fractal}$ is the moisture content (%) for the fractal part; D_i is one of the multi-fractal dimension values; and k_i is the corresponding constant to D_i. In this study, the D_i value was obtained from the average of all D values in each located group, and the lower point of each region, h, is defined as a critical point (h_c).

The D value could not be calculated from the *HA* model when h is below 0.4, approximately. It is speculated that this is probably because of the fact that at such low relative humidities, the wood internal surfaces may not have yet formed a ''fractal surface''; instead, they are just comprised of the discrete sorption sites. The description of these sites by a fractal concept is either impossible or quite difficult.

The classic BET model (Brunaner et al. 1938) predicts quite well wood sorption data below $h = 0.5$; thus it has been used extensively to estimate its two useful parameter values, namely, M_m and c, and to estimate the potential sorption area (Stamm 1964)

$$M_{non\text{-}fractal} = k\frac{M_m ch}{1 + ch} \tag{3}$$

Combining Eqs. (2) and (3), a new model, called the fractal polynomial (*FP*), can be obtained

$$M = k\frac{M_m ch}{1 + ch} + \sum k_i h^{D_i} \tag{4}$$

The *FP* model is similar to the polynomial sorption equation (7.80) in Siau (1995) in a fifth degree polynomial format and is claimed to provide, statistically, the best curve-fitness to sorption data. The *FP* model here used a noninteger power law, namely, fractal dimension, with an insightful physical meaning.

RESULTS AND DISCUSSION

Figure 1 shows the sorption isotherm for DFH specimens. Only the plots of DFH will be included in this paper due to space limitations; however, interested readers can find all pertinent plots for this study in Hao (2002). It can be seen that they exhibit the typical sigmoid curves (Type II) for wood, where the value of M decreases with an increase in temperature at the same relative humidity, and hysteresis is pronounced at each temperature level. This trend was apparent in all four types of specimens. There was no obvious difference between DFH and DFS regarding the M value at a corresponding h; however, a difference existed between RCH and E-RCH of about 3% of M at the high sorption regions.

The derivative plots (dM/dh) shown in Fig. 2 for DFH, were obtained for experimental points from the second lowest to the second highest of each of 24 sorption isotherms. The derivative for each calculated point was obtained by (moisture content$_{\text{its immediate upper point}}$ − moisture content$_{\text{its immediate lower point}}$)/($h_{\text{its immediate upper point}} - h_{\text{its immediate lower point}}$). The degree of inflection for a sorption curve can be revealed by a plot of dM/dh vs. h. In physical terms, it defines the rate of increase in M per unit increase in h. Through the higher sorption region, the moisture content increases, steadily, with an increase of h.

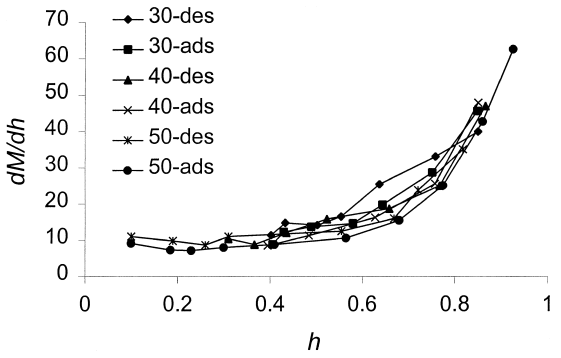

FIG. 2. The value of dM/dh for Douglas-fir heartwood.

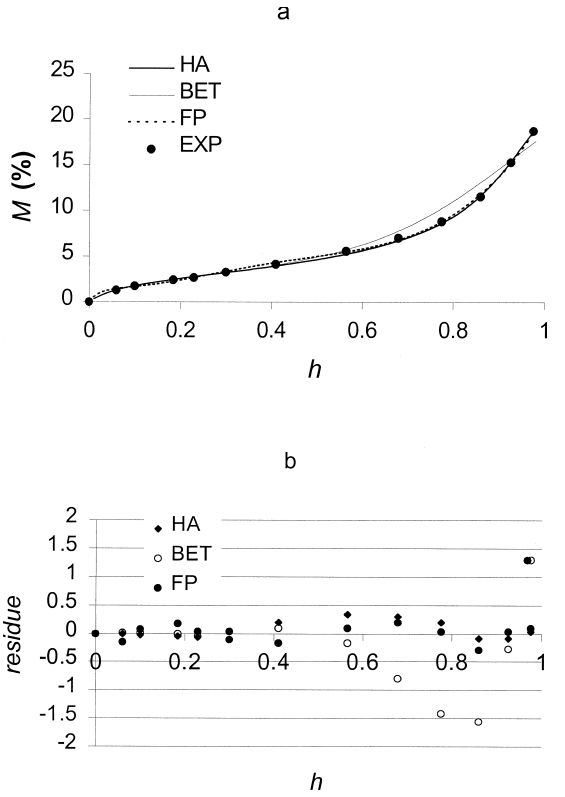

FIG. 3. The calculated adsorption isotherms (a) and their residue patterns (b) for Douglas-fir heartwood at 50°C.

It is well known that the classic BET equation with a finite number of layers of the sorbed water molecules cannot fit sorption data well mainly at a higher sorption region ($h > 0.5$) with few exceptions depending on the shape of the isotherm curves (Simpson 1973; Hartley 1994; Hao 1997). This trend was also clear in this study. For DFH at 50°C adsorption, the calculated plots of M vs. h from the classic BET were drawn with the *HA* and *FP* together in Fig. 3a. The respective regression residue patterns for each plot of M vs. h are shown in Fig. 3b. All other plots from the DFS, RCH, and E-RCH specimens and all temperature/sorption directions are not included here due to space limitations, however, they all show the same trends.

The residue pattern is a powerful tool along with the coefficient of determination (R^2) that indicates if a proposed equation fits the data well. If appropriate, the residue points should be uniformly, closely, and symmetrically distributed along the dependent variable-axis which in this study, is h-axis. The narrower the scattering band, the better the regression. The R^2 is a quantitative index that indicates if regression is appropriate, where the higher the value of R^2, the better the fit is. In the case of the calculated sorption isotherms, such an indication of R^2 was somehow misleading because the correlation coefficient between M and h was as high as 0.94. Although the BET model failed to fit the sorption data at the high sorption region in most cases in this study, it still produced significantly high R^2 values of 0.961 as shown in Table 1. Such high R^2 values are apt to give an incorrect conclusion on suitability of the tested equation. The failure of the BET model at high humidity sorption regions was similar in all types of wood used in this study. From this research, it can be noted that if the sorption isotherm curve was more inflectional (curvature) at the high sorption region, BET could not fit the sorption data (Fig. 3a)—it could fit otherwise. The reason for this is that its underlying assumption of being a flat sorption surface and the layering organization of the sorbed water may have deviated more from reality at these cases, thus resulting in a worse fit.

By assuming a non-flat surface within internal cell walls that results either from its origin or most probably caused by sorbed water

TABLE 1. *Parameter n estimation from the classic BET. (30d = desorption @ 30°C; 30a = adsorption @ 30°C).*

Species		30d	30a	40d	40a	50d	50a
DFH	*N*	10.080	12.580	10.188	13.480	10.330	12.92
	MSE	0.066	0.239	0.761	0.460	0.234	0.681
	R^2	0.998	0.994	0.979	0.988	0.993	0.981
DFS	*N*	8.841	12.110	9.630	12.380	9.960	12.05
	MSE	0.351	0.450	0.515	0.270	1.433	0.646
	R^2	0.989	0.989	0.996	0.994	0.966	0.982
RCH	*N*	8.433	11.930	8.453	13.620	11.135	11.3
	MSE	0.164	0.371	0.213	0.383	0.465	0.891
	R^2	0.994	0.987	0.991	0.987	0.986	0.961
E-RCH	*N*	9.119	12.060	9.610	12.690	11.021	12.193
	MSE	0.240	0.229	0.490	0.338	0.689	0.678
	R^2	0.994	0.994	0.988	0.991	0.985	0.976

molecules organized in some structure, the BET model was modified from the flat surface basis to the fractal surface one. The ensuing *HA* model was fitted to the sorption data, and the results are listed in Table 2 for all 24 test cases and drawn in Fig. 3a, with a thick solid line for DFH only. The residue pattern of each regression was coupled for each case.

It is apparent that *HA* fitted the sorption data better than BET did for each of 24 cases in this study. The largest *MSE* (mean square of error) value from the classic BET was 1.433, while it was 0.4277 from the *HA.* The *MSE* value was from 1 to 16 times less than that from the classic BET, depending on the inflection or the dM/dh rate of the sorption isotherm curve at the high sorption region. The greater the inflection, the better the improvement. The *MSE* is preferable to R^2 to facilitate comparison because R^2 values were so significantly high that the differences between the classic BET and *HA* models were not distinctive and an erroneous conclusion may thus be reached. The *HA* can fit the data well at both low and high humidities. The significantly improved degree of fit can be seen from the residue pattern at the high sorption region. The residue points came closer to the h-axis than those from the classic BET at high h levels for each of the 24 cases. The distribution of the residue points was more closely uniform and symmetrical to the h-axis. This suggests that the proposed equation is appropriate from the statistical point of view.

It should be noted here that the values in Table 2 were obtained by repeatedly fitting Eq. (1) to the different sorption regions from h of zero up to different h values. The above comparison is made from just the first line of each case. The results for all other lines were obtained based on the assumption that each h would produce a corresponding D value. Equation (1) was repeatedly fitted to the sorption data set with one fewer data points at a time until the results did not make sense or no longer related to the parameter D. All calculated D values and their corresponding h values are listed in Table 2. It can be seen that the D values became larger with an increase in h, and the value of n increased with an increase in h as well. The increase of D values with h was non-linear and in stepwise manner.

The derivation of the *FP* model, Eq. (4), was based on the assumption that the geometry of the internal cell-wall surfaces changed with h in a stepwise manner. The D values in Table 2 were averaged within one group in terms of the grouping guidelines. By using a linear regression technique, Eq. (4) was fitted to all experimental sorption isotherms in this study. The fitted results are listed in Table 3 for all twenty-four cases, and the derived sorption isotherm with the other two for DFH is presented in Fig. 3a and the residue pattern

TABLE 2. *The* D *values at the different sorption points from Eq. (1).*

	RCH				E-RCH				DFS				DFH			
	n	*MSE*	*h*	*D*	*n*	*MSE*	*h*	*D*	*n*	*MSE*	*h*	*D*	*n*	*MSE*	*h*	*D*
30d	12	0.14	0.91	2.33	14	0.13	0.91	2.35	15	0.27	0.91	2.45	14	0.05	0.91	2.27
	10	0.12	0.85	2.22	10	0.06	0.85	2.06	9	0.05	0.85	2.12	9	0.06	0.85	1.91
	7	0.04	0.76	1.90	9	0.04	0.76	2.12	9	0.04	0.76	2.15	7	0.05	0.76	1.61
	8	0.01	0.64	2.13	7	0.03	0.64	2.12	7	0.03	0.64	1.85	7	0.01	0.64	1.71
	7	0.01	0.55	1.77	7	0.04	0.55	1.78	9	0.02	0.55	1.90	7	0.01	0.55	1.53
	6	0.01	0.50	1.51	7	0.04	0.50	1.78	7	0.07	0.50	1.77	7	0.01	0.50	1.48
					6	0.02	0.43	1.70	7	0.04	0.43	1.73				
30a	24	0.12	0.97	2.43	15	0.21	0.97	2.29	22	0.16	0.97	2.38	18	0.14	0.97	2.26
	18	0.08	0.85	2.37	10	0.01	0.85	2.24	12	0.03	0.85	2.29	15	0.07	0.85	2.16
	12	0.03	0.75	2.18	10	0.01	0.75	2.20	12	0.04	0.75	2.24	12	0.04	0.75	2.01
	12	0.02	0.64	2.08	9	0.01	0.64	2.07	12	0.04	0.64	1.95	12	0.05	0.64	1.99
	12	0.03	0.58	2.06	7	0.00	0.58	2.01	7	0.01	0.58	1.70	9	0.02	0.58	1.80
	9	0.01	0.49	1.72	7	0.01	0.49	1.77	9	0.00	0.49	1.58	7	0.05	0.49	1.71
						0.01	0.43	1.49					7	0.09	0.43	1.62
40d	17	0.11	0.94	2.52	20	0.10	0.94	2.49	22	0.27	0.94	2.52	18	0.43	0.94	2.40
	12	0.04	0.86	2.39	12	0.04	0.86	2.42	12	0.02	0.86	2.31	12	0.03	0.86	2.27
	9	0.03	0.77	2.21	25	0.02	0.77	2.34	9	0.10	0.77	2.08	9	0.01	0.77	2.28
	8	0.03	0.66	2.20	7	0.01	0.66	2.32	9	0.11	0.66	2.12	9	0.02	0.66	2.07
	7	0.03	0.52	1.67	7	0.01	0.52	2.11	7	0.07	0.52	2.05	7	0.03	0.52	1.93
						0.01	0.44	1.82	6	0.04	0.44	1.98				
									5	0.09	0.37	1.67				
40a	30	0.10	0.94	2.40	23	0.09	0.94	2.36	22	0.11	0.94	2.36	25	0.05	0.94	2.35
	20	0.06	0.85	2.32	15	0.05	0.85	2.36	20	0.10	0.85	2.34	18	0.05	0.85	2.28
	20	0.05	0.76	2.27	9	0.03	0.76	2.14	12	0.03	0.76	2.10	9	0.02	0.76	2.09
	15	0.02	0.63	2.04	9	0.01	0.63	1.98	12	0.01	0.63	1.99	9	0.02	0.63	2.00
	12	0.02	0.48	1.71	5	0.01	0.48	1.77	9	0.02	0.48	1.53	9	0.04	0.48	1.53
50d	24	0.25	0.98	2.48	30	0.06	0.97	2.56	40	0.27	0.96	2.68	20	0.05	0.96	2.46
	18	0.04	0.90	2.43	22	0.04	0.91	2.51	18	0.02	0.90	2.55	16	0.02	0.82	2.36
	20	0.03	0.80	2.40	18	0.03	0.82	2.49	16	0.02	0.82	2.55	16	0.02	0.72	2.30
	16	0.01	0.70	2.30	7	0.02	0.70	2.34	9	0.01	0.70	2.29	9	0.00	0.67	1.86
	16	0.01	0.65	2.24	7	0.03	0.65	2.35	7	0.01	0.65	2.30	9	0.00	0.55	1.83
	14	0.01	0.53	2.04	5	0.00	0.53	2.04	7	0.02	0.53	2.01	7	0.00	0.31	1.84
	10	0.02	0.30	1.61	5				7	0.02	0.30	1.83	7	0.00	0.26	1.52
													5	0.00	0.19	1.43
50a	55	0.02	0.97	2.68	55	0.07	0.97	2.63	40	0.13	0.98	2.59	40	0.05	0.98	2.54
	30	0.01	0.89	2.68	30	0.07	0.86	2.58	40	0.07	0.90	2.63	40	0.04	0.93	2.55
	55	0.01	0.79	2.62	25	0.08	0.74	2.51	20	0.23	0.74	2.48	20	0.05	0.86	2.43
	30	0.01	0.66	2.62	40	0.09	0.66	2.45	15	0.02	0.66	2.40	15	0.04	0.78	2.37
	18	0.01	0.53	2.68	5	0.02	0.53	2.22	12	0.02	0.53	2.05	15	0.04	0.68	2.36
	14	0.02	0.40	2.13	40	0.00	0.40	2.15					9	0.03	0.57	2.04
	14	0.03	0.30	2.02									7	0.00	0.41	1.73
	14	0.03	0.23	1.36									7	0.00	0.30	1.87

Note: 30d and 30a same as in Table 1.

plotted in Fig. 3b. In most cases, the residue points for the twenty-four cases were more uniformly, symmetrically, and closely scattered around *h*-axis. It indicates that the *FP* model fitted the sorption data much better than the BET model. The *MSE* values from the *FP* model were mostly smaller than the ones from the *HA* one. The worst one was the classic BET equation due to its aforementioned problems at high relative vapor pressures.

The good fitness of the *FP* model strongly supported the assumption of the stepwise manner of the state of the sorbed water molecules. In Table 3, three steps were mainly identified

TABLE 3. *Fractal-Polynomial coefficient* (k_i) *estimations from Eq. (4).*

		RCH		E-RCH		DFS		DFH	
		D_i	k_i	D_i	k_i	D_i	k_i	D_i	k_i
30d		2.33	7581.02	2.35	170.49	2.45	519.28	2.27	428.66
		2.22	−13170.3	2.10	−211.53	2.13	−1414.00	1.91	−737.62
		2.02	6414.12	1.75	64.64	1.81	915.61	1.58	332.02
		1.64	−812.67	M_{mono}	23.39	M_{mono}	39.50	M_{mono}	18.39
		M_{mono}	39.40	0.03		0.10		0.01	
	MSE	0.03		1.00		1.00		1.00	
	R^2	1.00							
30a		2.40	13230.00	2.24	3207.00	2.38	1396.00	2.26	889.19
		2.11	−19280.00	2.04	−6870.00	2.27	100.66	2.05	−1363.00
		1.72	7505.00	1.63	5111.00	1.95	−1799.00	1.71	494.29
		M_{mono}	47.88	M_{mono}	73.18	1.64	425.02	M_{mono}	36.66
						M_{mono}	26.64		
	MSE	0.05		0.02		0.04		0.04	
	R^2	1.00		1.00		1.00		1.00	
40d		2.52	228.79	2.39	82580.00	2.52	306.68	2.40	835.67
		2.39	−277.52	2.11	−135700.00	2.31	−436.88	2.28	−1889.00
		2.21	64.84	1.82	72200.00	2.06	150.29	2.00	1074.00
		1.67	1003	M_{mono}	595.05	1.67	689.12	M_{mono}	24.47
		M_{mono}	18.53			M_{mono}	21.20		
	MSE	0.05		0.02		0.15		0.27	
	R^2	1.00		1.00		1.00		0.99	
40a		2.36	16450.00	2.36	675.24	2.35	288.16	2.35	390.39
		2.27	−26920.00	2.06	−1087.00	2.05	−386.00	2.28	−0.23
		2.04	13040.00	1.77	431.02	1.53	118.64	2.05	−520.41
		1.71	58.02	M_{mono}	20.55	M_{mono}	9.36	1.53	151.32
		M_{mono}	25.33					M_{mono}	14.39
	MSE	0.12		0.07		0.06		0.13	
	R^2	1.00		1.00		1.00		1.00	
50d		2.44	500.69	2.54	897.78	2.59	2735.00	2.46	2054.00
		2.27	240.93	2.39	−1277.00	2.30	−5023.00	2.33	−2760.00
		2.04	−276.93	2.04	399.54	2.01	2594.00	1.76	1030.00
		1.61	53.28	M_{mono}	13.07	1.83	78.55	M_{mono}	26.62
		M_{mono}	8.98			M_{mono}	77.61		
	MSE	0.17		0.07		0.39		0.02	
	R^2	0.99		1.00		0.99		1.00	
50a		2.66	129.01	2.57	152.31	2.61	656.29	2.54	5324.00
		2.07	−184.19	2.45	1617.00	2.44	−907.34	2.39	−8994.00
		1.36	73.92	2.22	−2068.00	2.05	269.75	2.04	5599.00
		M_{mono}	−7.76	2.15	469.45	M_{mono}	5.95	1.80	−1915.00
				M_{mono}	7.99			M_{mono}	29.30
	MSE	0.14		0.08		0.18		0.02	
	R^2	0.99		1.00		0.99		1.00	

Note: 30d and 30a same as in Table 1.

for the determination of a better sorption isotherm. This implied that at least three fractal values were needed to characterize the sorption property. These three sorption stages can be seen in Fig. 2, where dM/dh plots can roughly be separated into three regions from low to high humidity levels. Traditionally, these three regions are considered to coincide with chemical sorption, molecular re-organization, and physico-sorption according to Hartley et al. (1992) and Hartley and Avramidis (1993). These ranges are considered in the classic BET theory to be the area of monolayer formation, a transition of the monolayer to

multilayer, and the multilayer area, respectively. In terms of the *D* values at different stages, the spatial distribution of the sorbed water molecules may have changed from something between a line and a plane, and transition near to a plane, and then toward a spatial distribution (far from a plane with a limit of 2.7 of *D*). The corresponding moisture content ranges for these groups were about 5–9%, 10–15%, and 16–20% or above.

Fundamentally, the *HA* and *FP* models are physically similar from a fractal point of view, even though they have totally different formats. The *HA* quantifies the geometry of the internal surfaces of the cell walls, which are considered to be shaped by the geometry of the sorbed water molecules. If the former is considered to be the same as the latter, both equations can be considered to quantify the geometry of the same complex object from different angles, namely, either from the network of the sorbed water molecules or from the internal surfaces of the cell walls.

CONCLUSIONS

In the light of this investigation, the following conclusions can be drawn:

1) Failure of the classic BET theory to predict the vapor sorption levels in wood at the high sorption regions ($h > 0.5$) can be attributed to the existence of a geometrically rough substrate surface with a *D* value from about 2.3 to 2.6. The geometry with *D* values of this range is far from being described as a flat surface ($D = 2$).
2) A new sorption theory with its equation was developed and evaluated. It considered both the molecular layering stage at low humidity and the non-layering or fractal sorption stages at high humidity. Its good curve-fitness justified the assumption that the state dynamics of the sorbed water were stepwise or locative instead of continuously smooth and 3 or 4 steps were identified.

REFERENCES

BRUNANER, S., P. H. EMMETT, AND E. TELLER. 1938. Adsorption of gases in multilayer. J. Am. Chem. Soc. 60: 309–319.

HAO, B. 1997. Moisture sorption characteristics of five B.C. softwoods. Directed Study Report. Department of Wood Science, The University of British Columbia, Vancouver, BC, Canada.

———. 2002. Fractal geometry of wood internal surfaces in the hygroscopic range. Ph.D. thesis, Department of Wood Science, The University of British Columbia, Vancouver, BC, Canada.

———, AND B. AVRAMIDIS. 2001. Wood sorption fractality in the hygroscopic range, part I. Evaluation of a modified classic BET model. Wood Fiber Sci. 33(1): 119–125.

HARTLEY, I. D. 1994. Characterization of water in wood below the fiber saturation point. Ph.D. thesis, The University of British Columbia, Department of Wood Science, Vancouver, BC, Canada.

———, AND S. AVRAMIDIS. 1993. Analysis of the wood sorption isotherm using clustering theory. Holzforschung 47(2):163–167.

———, F. A. KAMKE, AND H. PEEMOELLER. 1992. Cluster theory for water sorption in wood. Wood Sci. Technol. 26(2):83–99.

KELSEY, K. 1957. The sorption of water vapor by wood. Aust. J. Appl. Sci. 8(1):42–54.

SIMPSON, W. 1973. Predicting equilibrium moisture content of wood by mathematical models. Wood Fiber 5(1): 41–49.

SIAU, J. F. 1984. Transport processes in wood. Springer-Verlag, Berlin, Heidelburg, New York.

SIAU, J. F. 1995. Wood: Influence of moisture content on wood properties. Virginia Polytechnic Institute and State University, Blacksburg, VA. 245 pp.

STAMM, A. J. 1964. Wood and cellulose science. Ronald Press, New York, NY. 550 pp.